Advent of Diamond Electronics:

Dr. James E. Butler

- Leading Scientist, Institute of Applied Physics, Nizhny Novgorod, Russian Academy of Sciences, and St. Petersburg Electrotechnical University (LETI), Russian Ministry of Science and Education ‘Mega grant’ 2013 - 2017
- Consultant, Cubic Carbon Ceramics, Huntingtown, MD 20639
- Vice President, Diamond Technology, Euclid Techlabs LLC, Gaithersburg, MD
- Chief Scientist/co-Founder, Diamond Foundry, San Francisco, CA
- Research Associate, Smithsonian National Museum of Natural History, Washington DC
- Visiting Scientist, Dept. of Physics, Vanderbilt University,
- Adjunct Fellow, Macquarie University, Sydney Australia

Jimbutler29@comcast.net

Motivation
Challenges
Progress

Comparative Material Properties (for Electronic Applications)

Material	Eg	ε	μ	Ec	vsat	λ	ni
	eV		cm2/Vs	10^6 V/cm	10^7 cm/s	W/cmK	cm-3
Si	1.1	11.8	1350	0.3	1	1.5	1.50E+10
Ge	0.66	16	3900	0.1	0.5	0.6	2.40E+13
GaAs	1.4	12.8	8500	0.4	2	0.5	1.80E+06
GaP	2.3	11.1	350	1.3	1.4	0.8	7.70E-01
GaN	3.39	9	900	3.3	2.5	1.3	1.90E-10
3C-SiC	2.2	9.6	900	1.2	2	4.5	6.90E+00
4H-SiC - a axis	3.26	10	720	2	2	4.5	8.20E-09
4H-SiC - c axis	3.26	10	650	2	2	4.5	8.20E-09
6H-SiC - a axis	2.86	9.7	370	2.4	2	4.5	2.40E-05
6H-SiC - c axis	2.86	9.7	50	2.4	2	4.5	2.40E-05
Diamond	5.45	5.5	1900	5.6	2.7	20	1.60E-27
CVD Diamond	5.45	5.5	3800	10	2.8	22	1.60E-27
AlN	5.61	8.7	1100	1.2	1.8	1.7	

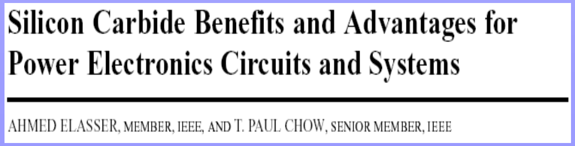

Silicon Carbide Benefits and Advantages for Power Electronics Circuits and Systems

AHMED ELASSER, MEMBER, IEEE, AND T. PAUL CHOW, SENIOR MEMBER, IEEE

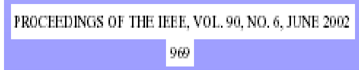

PROCEEDINGS OF THE IEEE, VOL. 90, NO. 6, JUNE 2002

969

Revised Figures of Merit

basic limit on the device performance

Power Density & transistor switching speed

Thermal properties, heat sink

Low-frequency Resistive Losses

High-frequency switching losses

Material	JM	MJM	KM	Qf1	Qf2	BM(Qf3)	BHFM
	$\left(E_c v_{sat} \pi^{-1}\right)^2$	$\lambda \cdot \mathrm{JM}$	$\lambda \sqrt{v_{sat} \varepsilon^{-1}}$	$\lambda \sigma_A$	$\lambda \sigma_A E_c$	$\sigma_A = \varepsilon \mu E_c^3$	μE_c^2
Si	1	1	1	1	1	1	1
Ge	0.03	0.01	0.24	0.06	0.02	0	0.32
GaAs	7	2	0	5	7	16	11
GaP	37	20	1	11	46	20	5
GaN	756	655	2	587	6454	677	81
3C-SiC	64	192	5	104	417	35	11
4H-SiC - a axis	178	533	5	402	2679	134	24
4H-SiC - c axis	178	533	5	363	2419	121	21
6H-SiC - a axis	256	768	5	346	2769	115	18
6H-SiC - c axis	256	768	5	47	374	16	2
Diamond	2540	33870	32	56905	1062227	4268	490
CVD Diamond	8712	127769	36	712868	23762274	48605	3128
AlN	52	59	2	44	174	38	13

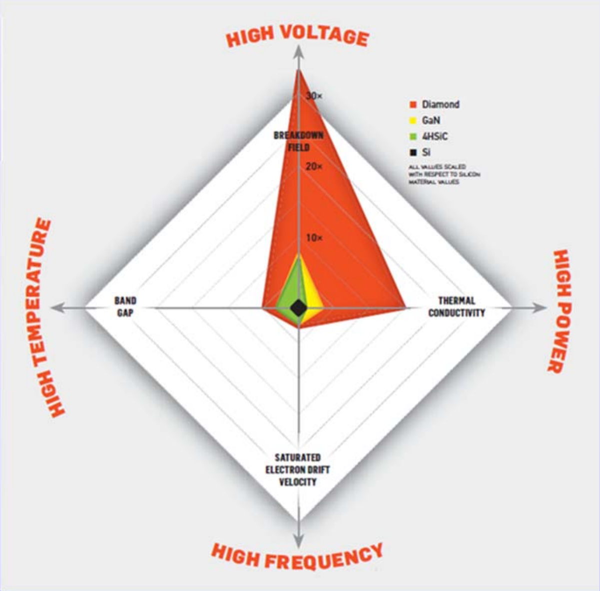

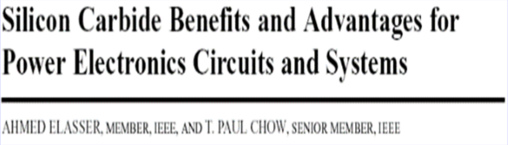

Silicon Carbide Benefits and Advantages for Power Electronics Circuits and Systems

AHMED ELASSER, MEMBER, IEEE, AND T. PAUL CHOW, SENIOR MEMBER, IEEE

PROCEEDINGS OF THE IEEE, VOL. 90, NO. 6, JUNE 2002

969

From: www.egr.msu.edu/fraunhofer-ccd/

Probable Applications for Diamond Electronics

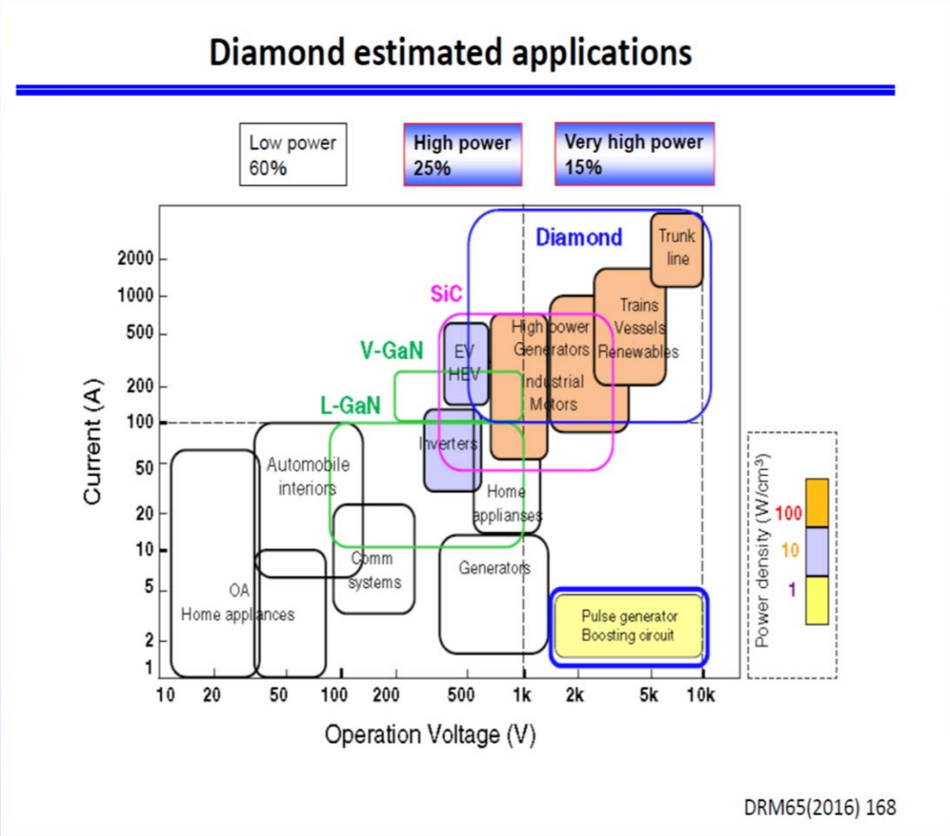
Diamond estimated applications

DRM65(2016) 168

S-i. Shikata – AIST Japan

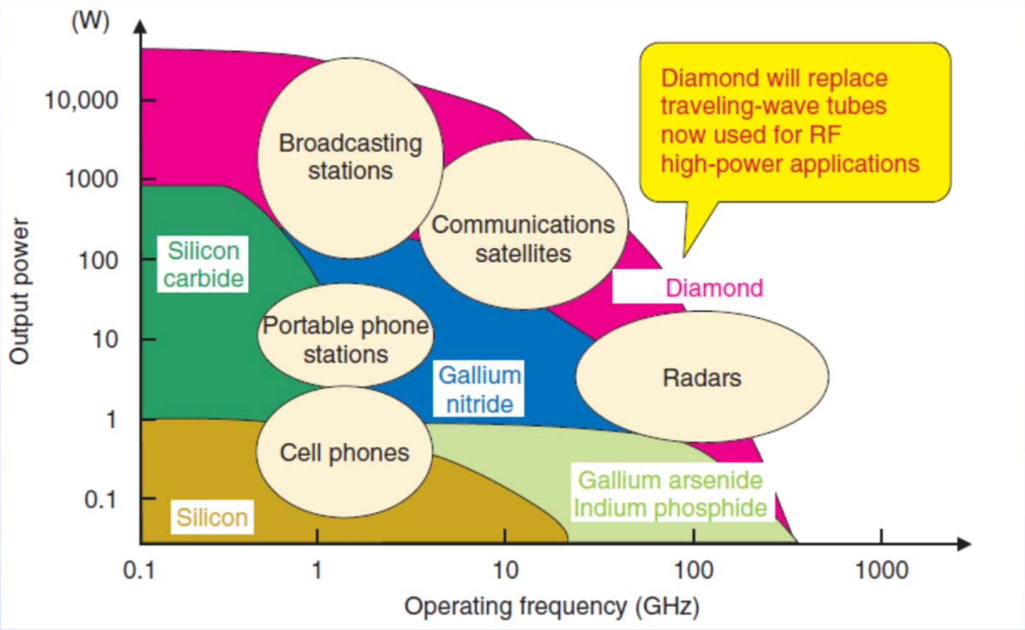

Diamond will replace traveling-wave tubes now used for RF high-power applications

M. Kasu, NTT Tech. Review,

Requirements for Diamond Electronics

- Need charge carriers
  - Electrons in conduction band
  - Holes in valance band
- Need High Mobility
- Need high breakdown strength
- Need High thermal diffusivity
- Cost Effective Production

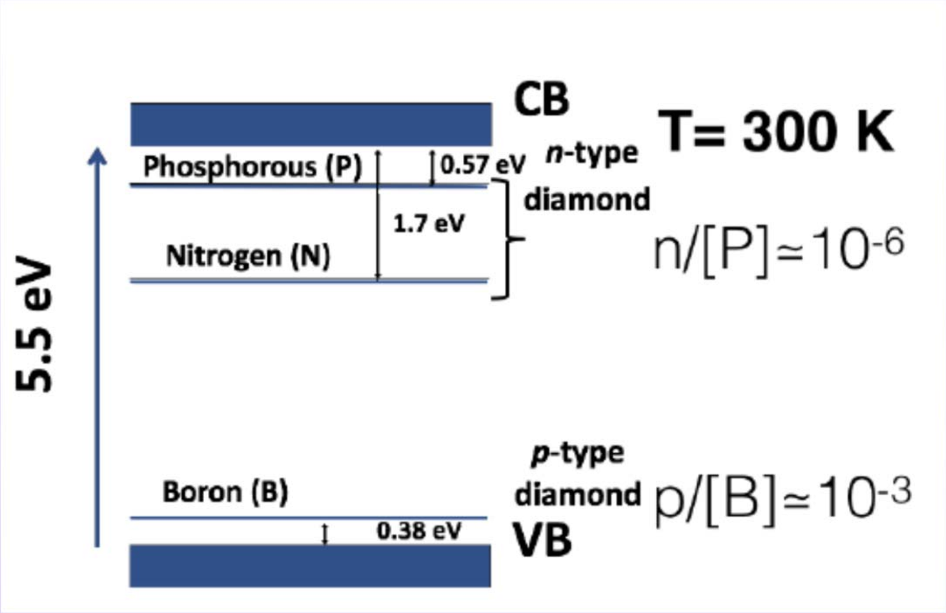

Traditional Issues Limiting Diamond Electronics

- Impurities and Defect structure
  - Natural Diamonds – Lack on Uniformity: "they are like snowflakes, no 2 are identical"
    - N impurities
    - dislocations
  - HPHT
    - N, Metal solvent impurities
    - Dislocations
  - CVD
    - Dependent on substrate seed crystallography
    - Good control of purity
- Doping – electrically active impurities
  - Few atoms are small enough to fit into diamond lattice
    - B, N, H, Si, Ni, …
    - Electrically active dopants are energetically removed from the conduction or valance bands
- Size and Availability for mass market

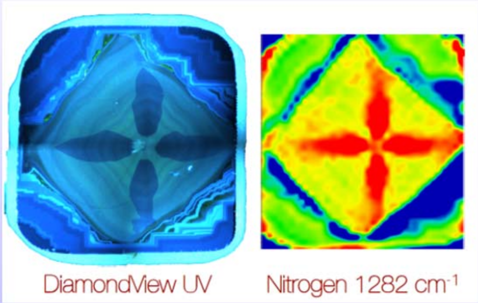
DiamondView UV
Nitrogen 1282 cm^{-1}

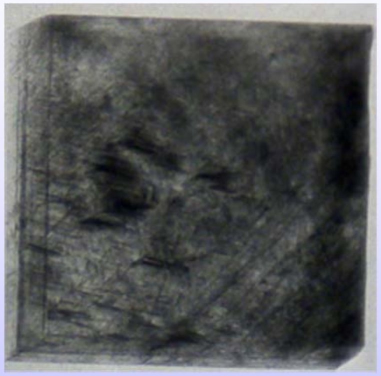

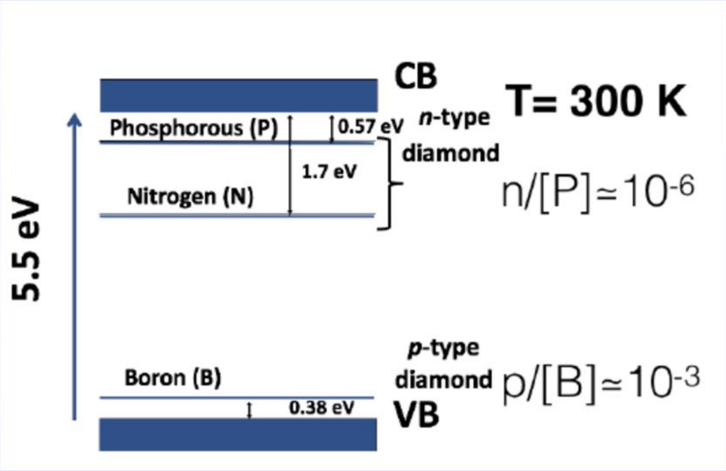

Diamond as a Semiconductor

Creating Charge Carriers in Diamond

- Bulk Doping
  - P-type - Boron 0.37 eV
  - N-type - Phosphorous 0.6 eV
- Surface Doping
  - P-type - surface adsorbate creates 2D hole gas in subsurface region
- “Delta Doping”
- Vacuum Electronics
- Photo carrier generation
- Quantum Electronics and Sensors

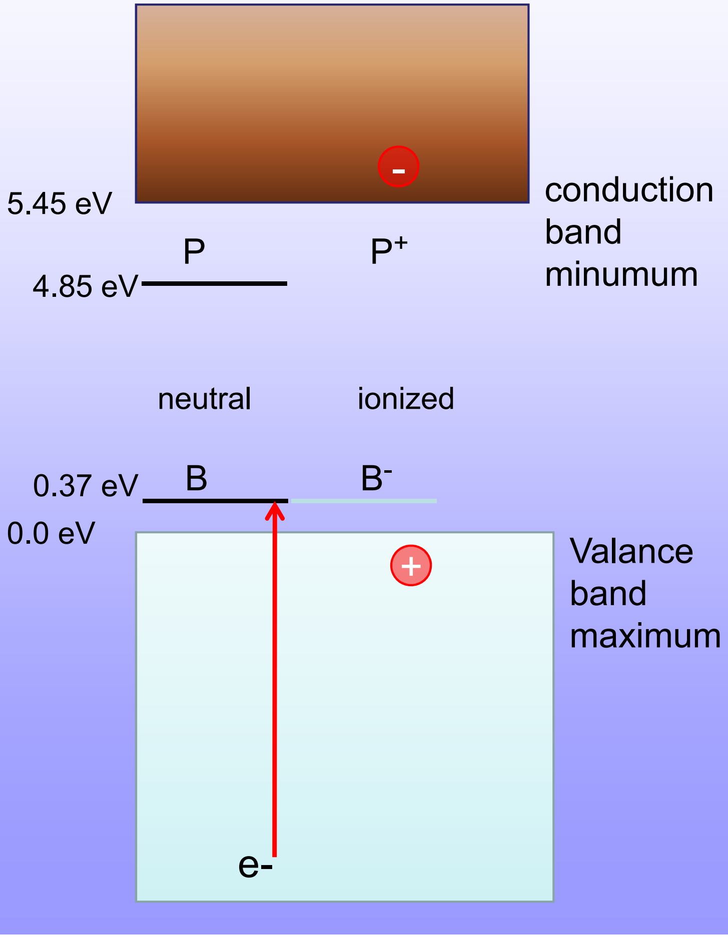

Doping diamond with Boron (bulk)

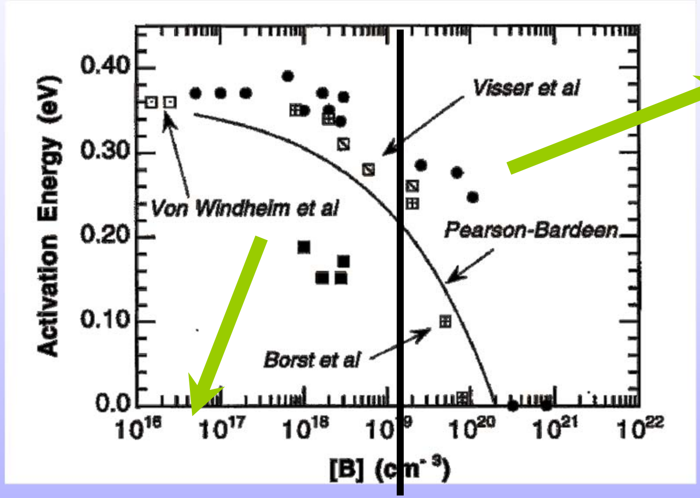

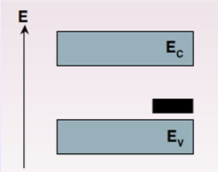

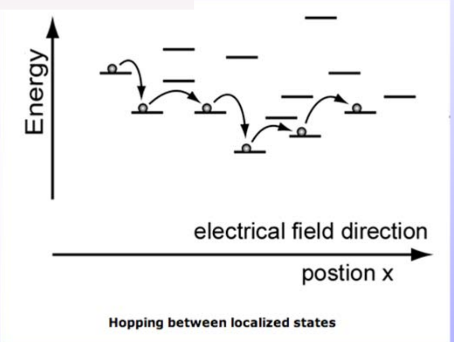

Hopping between localized states

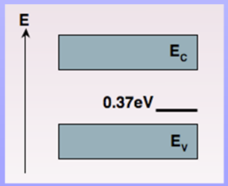

Impurity band formation, hopping conduction, low mobility
Requires little thermal activation
Conductivity at room temperature

Discrete acceptor state, band conduction, high mobility
Requires high activation energy
Little conductivity at room temperature

Activation energy graph from
Borst & Weiss, Phys. Stat. Sol., A154, 423 (1996)

Carrier Concentration

Room temperature

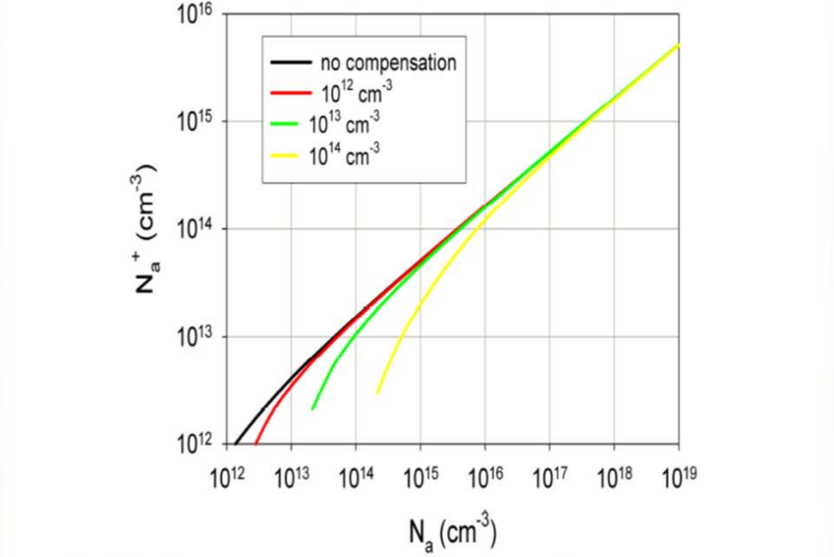

FIGURE 1. *Hole concentration vs. dopant concentration of boron doped diamond at room temperature for different concentrations of compensating donors. At higher boron concentrations higher than* 10^{19} *cm*$^{-3}$ *the activation increases rapidly to full activation and conduction becomes metallic-type.*

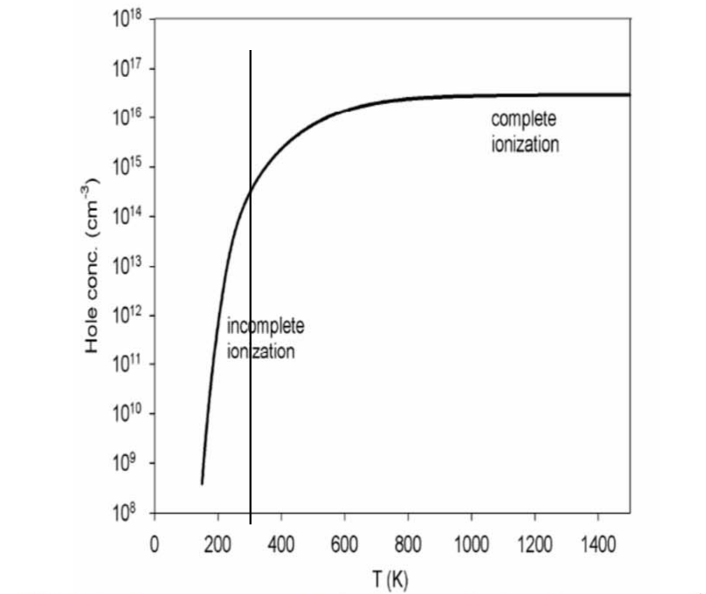

FIGURE 2. *Hole concentration vs. temperature of boron doped diamond with dopant concentration* $N_A = 4 \cdot 10^{16}$ *cm*$^{-3}$ *and compensating donor concentration* $N_D = 2 \cdot 10^{14}$ *cm*$^{-3}$.

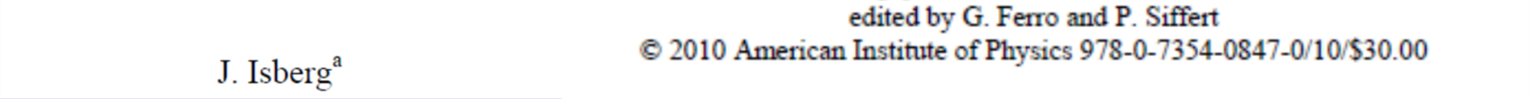

Diamond Electronic Devices

J. Isberg[a]

CP1292, *2010 Wide Bandgap Cubic Semiconductors: From Growth to Devices*
edited by G. Ferro and P. Siffert

Hall Mobility

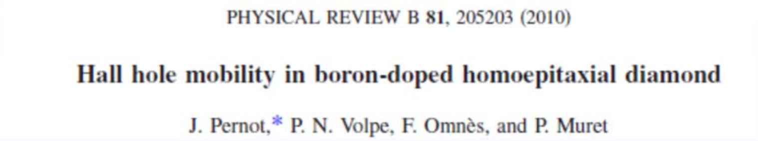

PHYSICAL REVIEW B **81**, 205203 (2010)

Hall hole mobility in boron-doped homoepitaxial diamond

J. Pernot,* P. N. Volpe, F. Omnès, and P. Muret

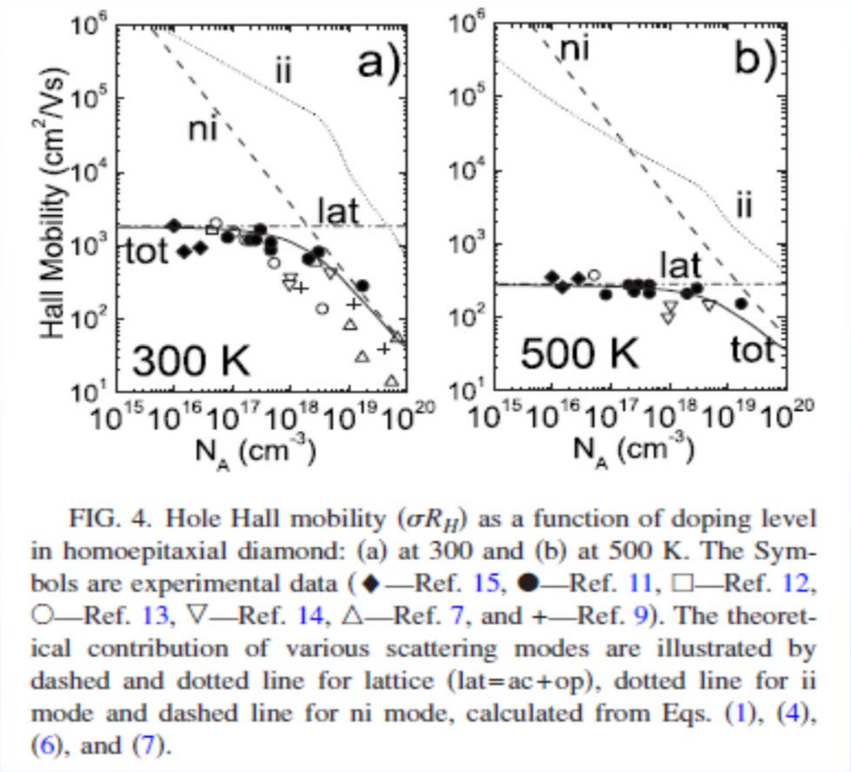

FIG. 4. Hole Hall mobility (σR_H) as a function of doping level in homoepitaxial diamond: (a) at 300 and (b) at 500 K. The Symbols are experimental data (◆—Ref. 15, ●—Ref. 11, □—Ref. 12, ○—Ref. 13, ▽—Ref. 14, △—Ref. 7, and +—Ref. 9). The theoretical contribution of various scattering modes are illustrated by dashed and dotted line for lattice (lat=ac+op), dotted line for ii mode and dashed line for ni mode, calculated from Eqs. (1), (4), (6), and (7).

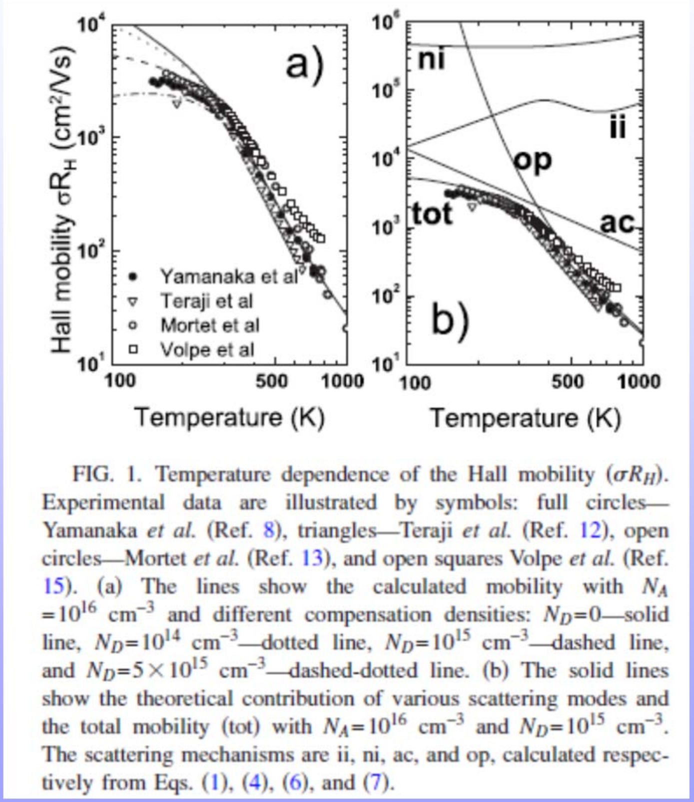

FIG. 1. Temperature dependence of the Hall mobility (σR_H). Experimental data are illustrated by symbols: full circles—Yamanaka *et al.* (Ref. 8), triangles—Teraji *et al.* (Ref. 12), open circles—Mortet *et al.* (Ref. 13), and open squares Volpe *et al.* (Ref. 15). (a) The lines show the calculated mobility with $N_A = 10^{16}$ cm^{-3} and different compensation densities: $N_D = 0$—solid line, $N_D = 10^{14}$ cm^{-3}—dotted line, $N_D = 10^{15}$ cm^{-3}—dashed line, and $N_D = 5 \times 10^{15}$ cm^{-3}—dashed-dotted line. (b) The solid lines show the theoretical contribution of various scattering modes and the total mobility (tot) with $N_A = 10^{16}$ cm^{-3} and $N_D = 10^{15}$ cm^{-3}. The scattering mechanisms are ii, ni, ac, and op, calculated respectively from Eqs. (1), (4), (6), and (7).

Above MIT ($N_a > 4x10^{20}$ cm^{-3}
Mobility = 3-5 cm^2/Vsec

Delta Doping of Diamond with Boron

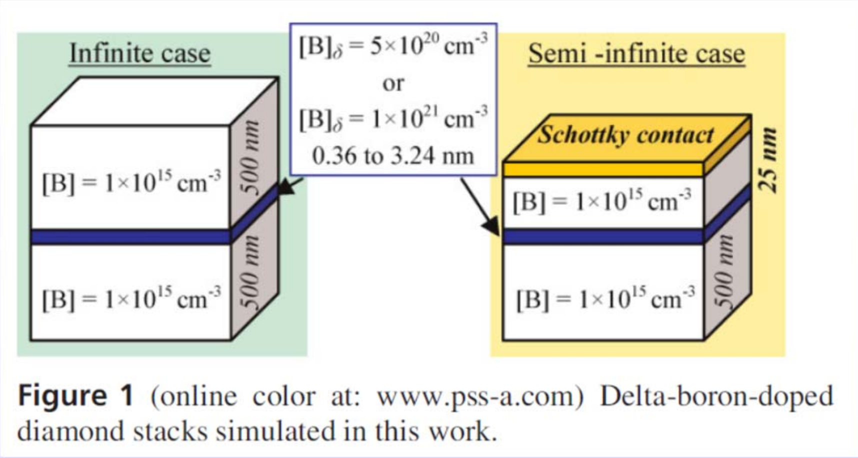

Figure 1 (online color at: www.pss-a.com) Delta-boron-doped diamond stacks simulated in this work.

Simulations of carrier confinement in boron δ-doped diamond devices

Alexandre Fiori*, Julien Pernot, Etienne Gheeraert, and Etienne Bustarret**

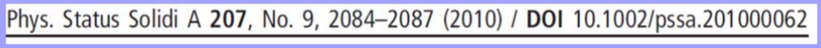

Phys. Status Solidi A **207**, No. 9, 2084–2087 (2010) / **DOI** 10.1002/pssa.201000062

Carrier density vs distance

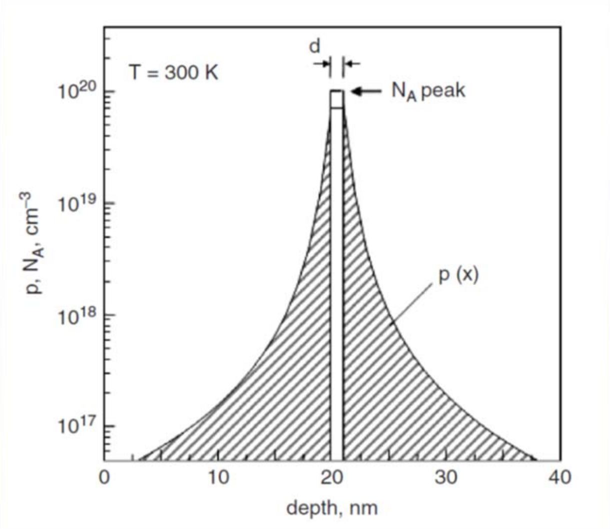

E. Kohn and A. Denisenko
p. 319 in *“CVD Diamond for Electronic Devices and Sensors”*
Ed. R.S. Sussmann

Delocalization of Holes

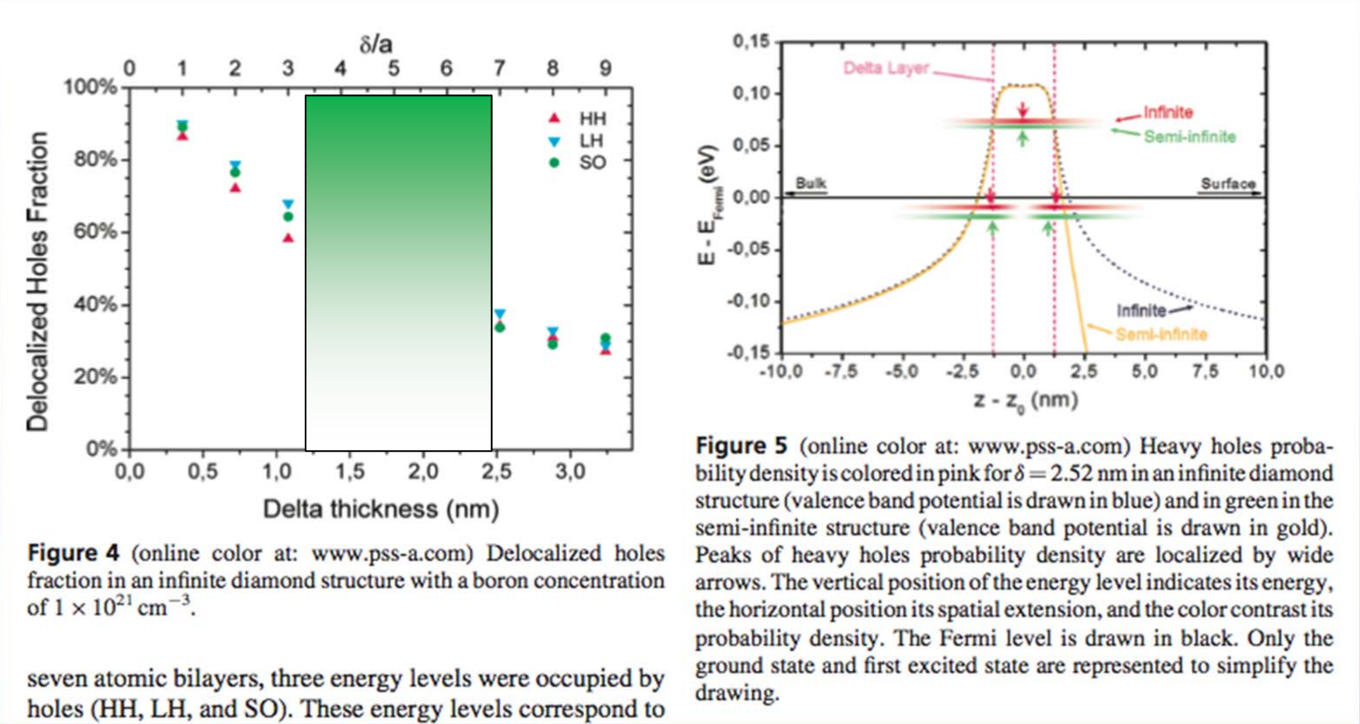

Figure 4 (online color at: www.pss-a.com) Delocalized holes fraction in an infinite diamond structure with a boron concentration of $1 \times 10^{21}\,\mathrm{cm}^{-3}$.

seven atomic bilayers, three energy levels were occupied by holes (HH, LH, and SO). These energy levels correspond to

Figure 5 (online color at: www.pss-a.com) Heavy holes probability density is colored in pink for $\delta = 2.52$ nm in an infinite diamond structure (valence band potential is drawn in blue) and in green in the semi-infinite structure (valence band potential is drawn in gold). Peaks of heavy holes probability density are localized by wide arrows. The vertical position of the energy level indicates its energy, the horizontal position its spatial extension, and the color contrast its probability density. The Fermi level is drawn in black. Only the ground state and first excited state are represented to simplify the drawing.

Simulations of carrier confinement in boron δ-doped diamond devices

Alexandre Fiori*, Julien Pernot**, Etienne Gheeraert, and Etienne Bustarret

Phys. Status Solidi A **207**, No. 9, 2084–2087 (2010) / **DOI** 10.1002/pssa.201000062

Delta-doping:
Mobility of previous experiments

- Other materials- enhancement:
  - GaAs, GaN – mobility 2D structures even higher than in 3D

- Diamond (other research groups 2000-now): no enhancement

French group: [G. Chicot et al. Appl. Phys. Lett. 101, 162101 (2012)]
[G. Chicot et al. J.Appl.Phys., 116, 083702(2014)]

Mobility = 3.6 (0.8) cm^2/Vsec

E6+Germany: [H. El-Hajj et al, DRM, 17, 2008, 409]
[J. Scharpf et al. Physica Status Solidi a-Applications and Materials Science 2013, 210, 2028]

Mobility = 0.01 to 0.1 cm^2/Vsec

Element 6: [R. S. Balmer et al. Journal of Applied Physics 2013, 113.]

Mobility = 3.8 cm^2/Vsec

OUR STRATEGY

- High Quality, low dislocation density HPHT (100) substrates
- Polish to 0.1 to 0.3 nm Ra
- Remove polishing damage
- Design ultra fast gas switching laminar flow CVD reactor
- Grow smooth epilayers VERY slowly, ca. 30 to 70 nm/hr
- Chemically getter residual boron contamination during growth of intrinsic layers

Substrate preparation for atomically smooth surface

1. **Polishing of substrate, single crystal (100) diamond (Ra < 0.3 nm)**

80 x80 microns
Sa = 0.15 nm
Sq = 0.19 nm

Zygo Opt. Interferometer

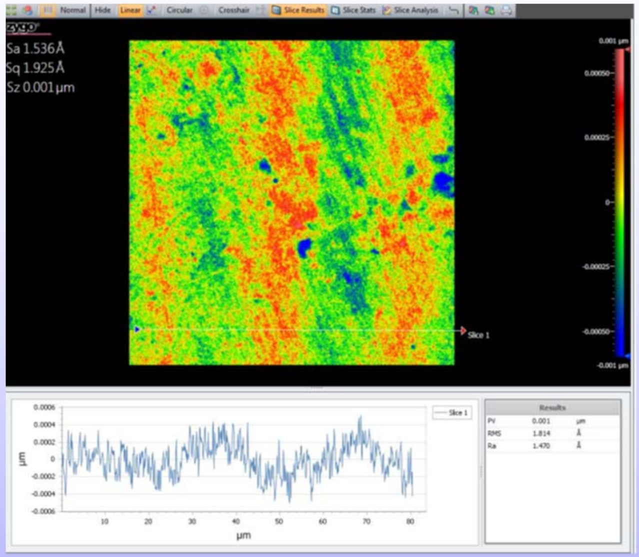

Sa 1.536Å
Sq 1.925Å
Sz 0.001µm

Results		
PV	0.001	µm
RMS	1.814	Å
Ra	1.470	Å

2. ICP(Inductively coupled plasma)-RIE etching

ICP etching of diamond is highly homogeneous, does not increase surface roughness and eliminate polishing damages.

[A.B. Muchnikov et al., Phys. Status Solidi A, 2015]

3. Surface after CVD growth, Ra<0.25 nm

2x2 microns
AFM

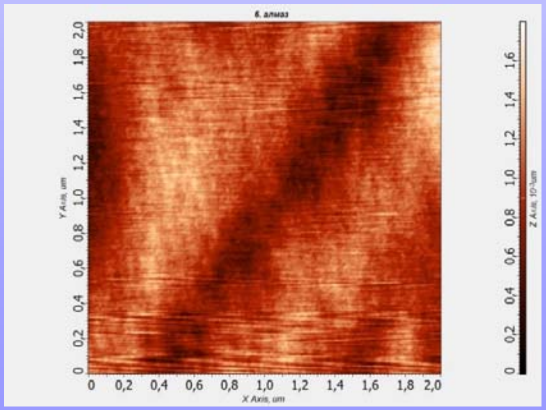

Main features of delta doping reactor

1. Rapid gas switching allows achieving fast changing of gas mixtures containing B_2H_6 and without B_2H_6

2. Laminar gas flow in reactor – vortexes and stagnant regions are absent

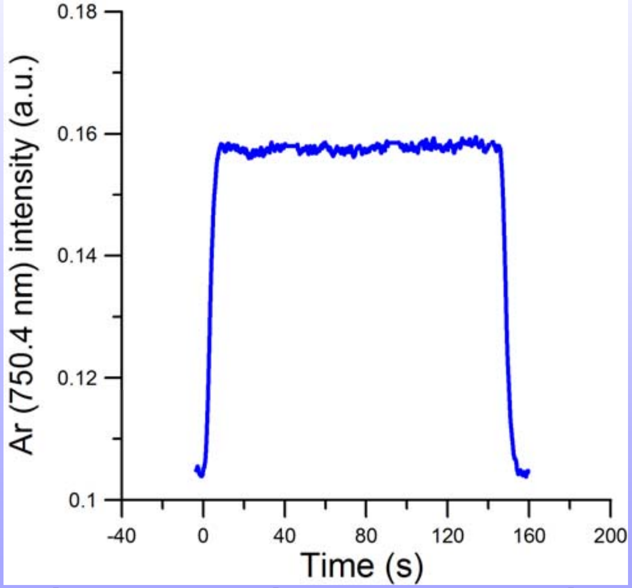

Intensity of Ar (added in diagnostic purposes) line on time after changing gas mixture from H_2-CH_4 to H_2-CH_4-Ar and back. Total gas flow 950 sccm.

3. Axial symmetric resonant mode – symmetric discharge

4. Slow growth of diamond 40-100 nm/h
low methane content <0.1%, low pressure 40 Torr

TEM measurements

Interfaces are barely seen, full epitaxy.

substrate

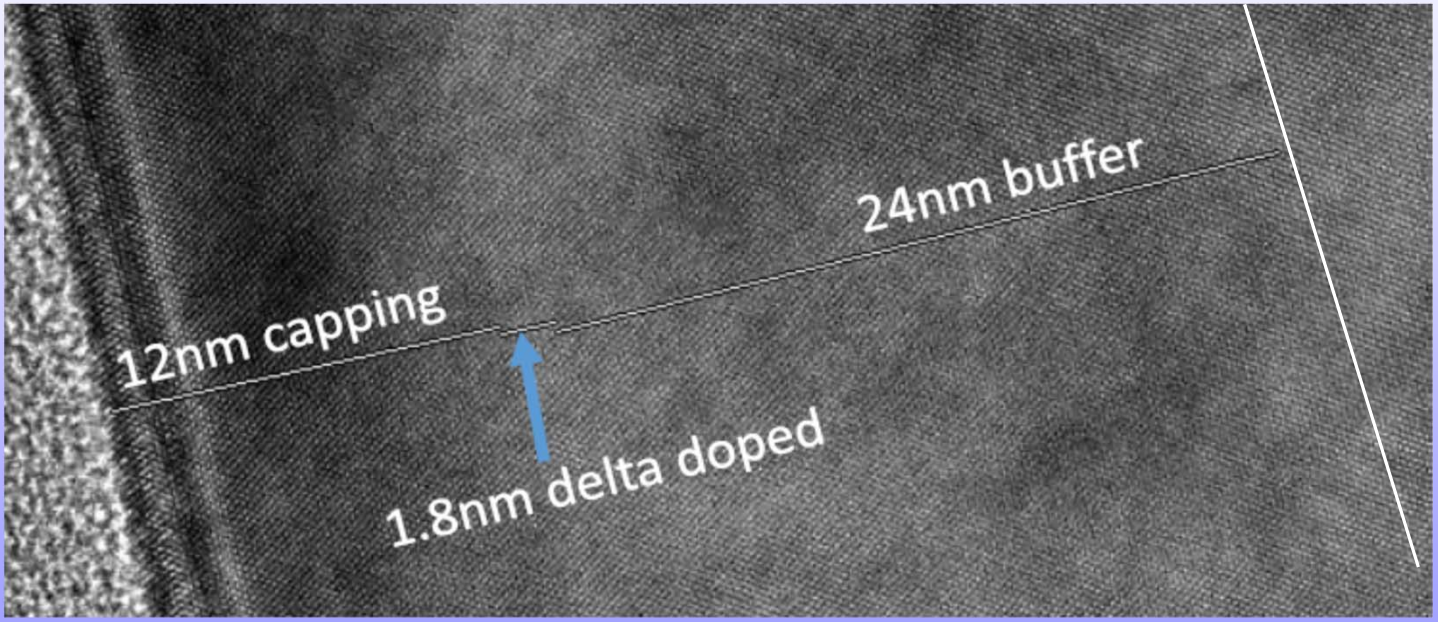

CVD deposition

SIMS sputter profiling

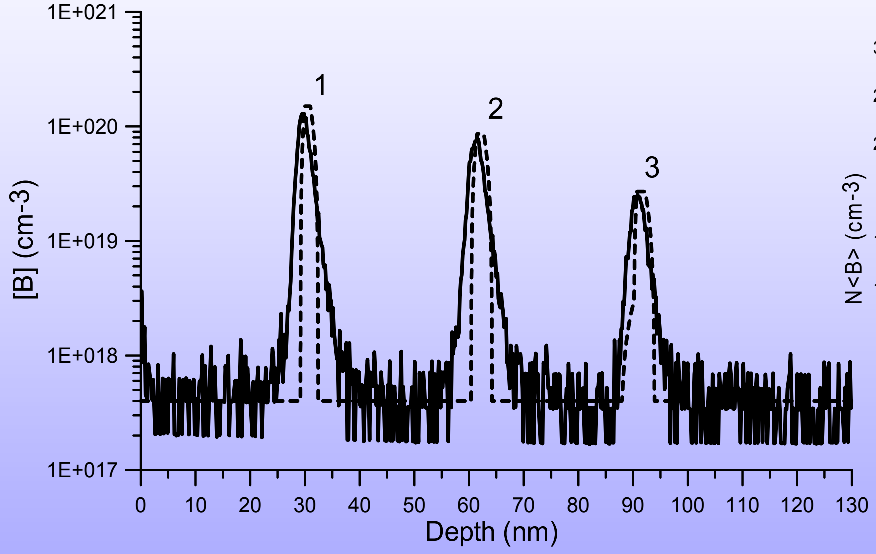

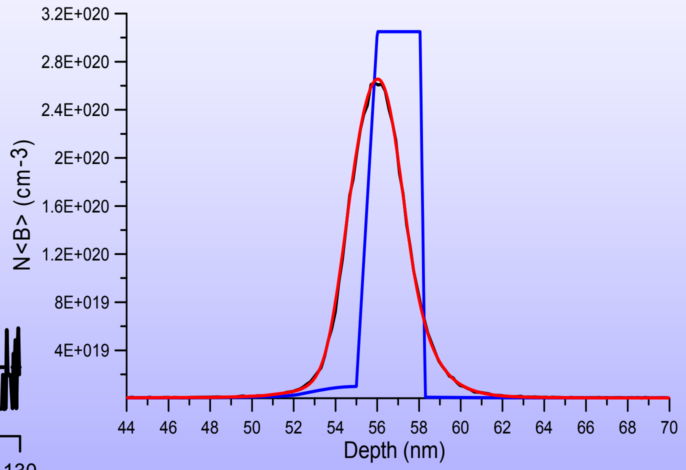

Deconvolute SIMS Instrument function:
S. Hofmann, Y. Liu, J. Y. Wang, J. Kovac,
Applied Surface Science 2014, 314, 942.

CV of vertical mesa with delta layers

Formation of the mesa structure with contact to the bottom P$^+$ layer

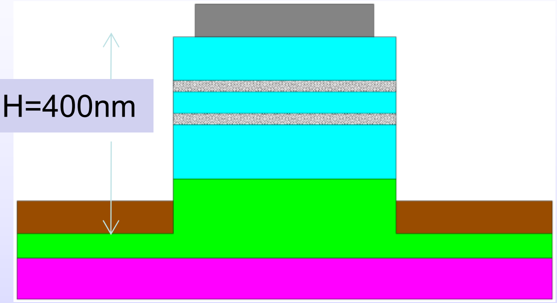

- ▨ Delta layers
- 🟦 Non doped diamond
- 🟩 Heavily doped p$^+$ diamond
- 🟪 Diamond substrate
- 🟫 Ohmic contact
- ⬛ Schottky contact

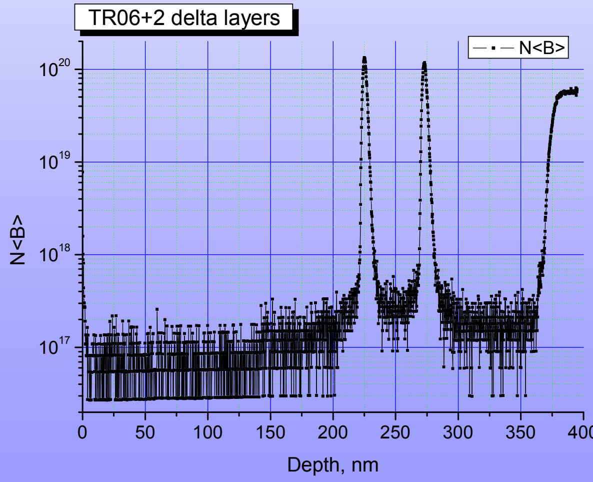

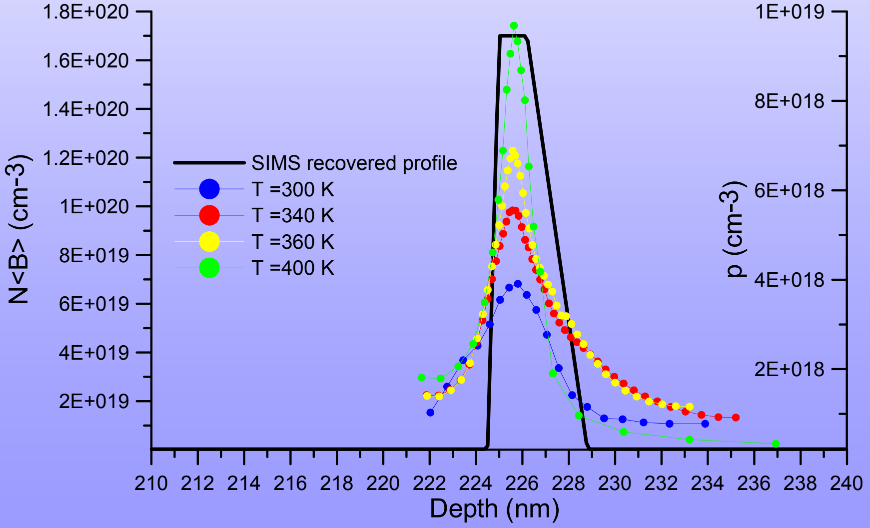

Previous Hall Measurements

(vdp and Hall bar)

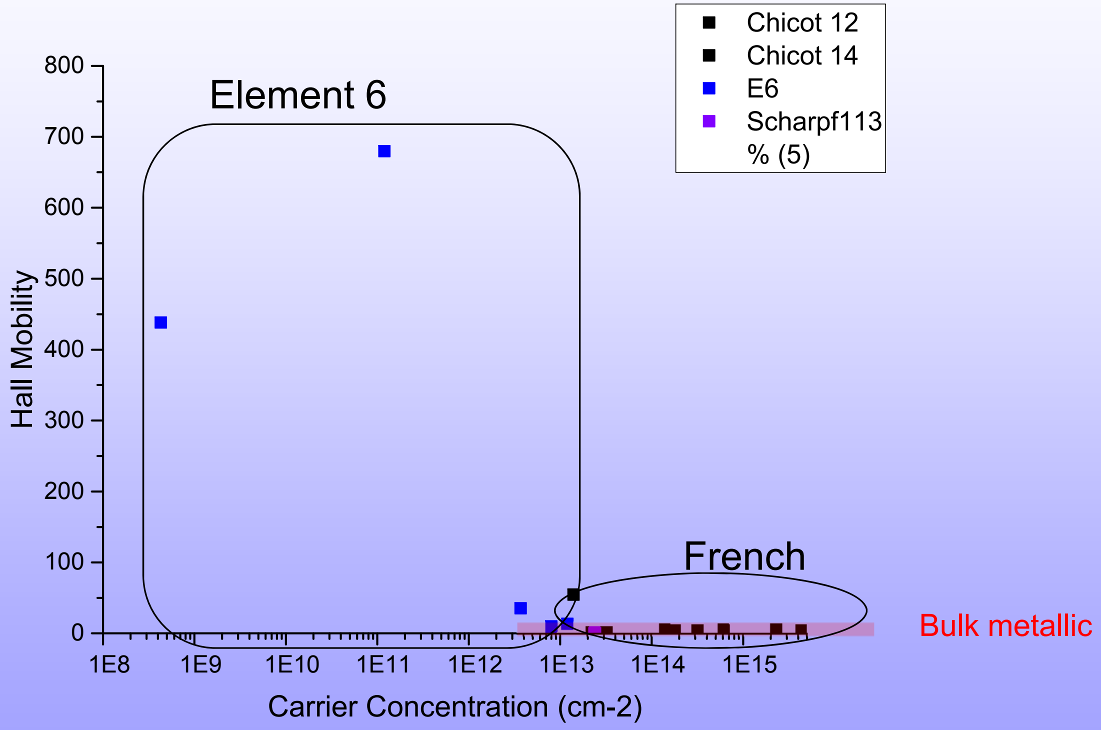

Initial Hall Measurements

(vdp config.)

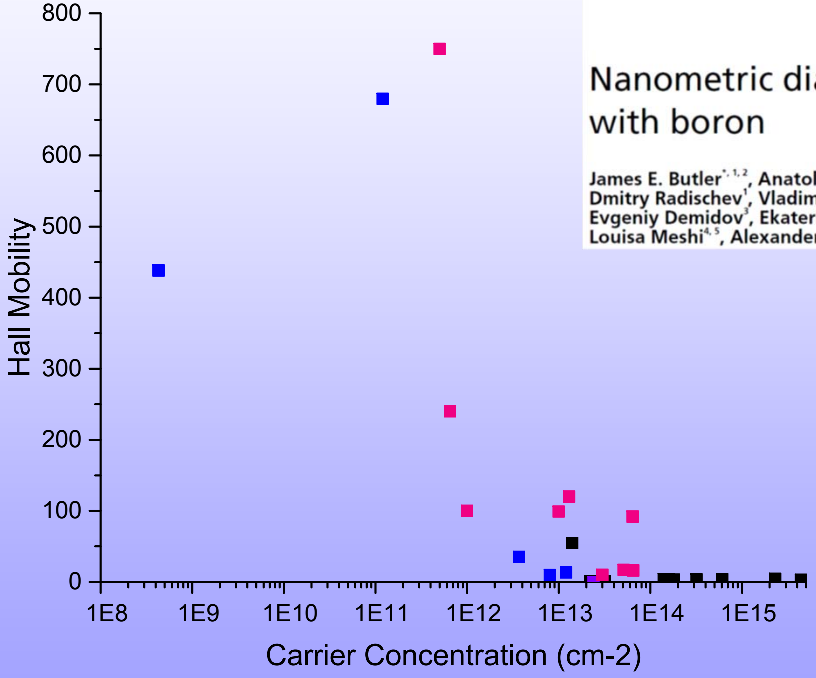

Phys. Status Solidi RRL **11**, No. 1, 1600329 (2017) / **DOI** 10.1002/pssr.201600329

Nanometric diamond delta doping with boron

James E. Butler[*, 1, 2], Anatoly Vikharev[1], Alexei Gorbachev[1], Mikhail Lobaev[1], Anatoly Muchnikov[1], Dmitry Radischev[1], Vladimir Isaev[1], Valerii Chernov[1], Sergey Bogdanov[1], Mikail Drozdov[3], Evgeniy Demidov[3], Ekaterina Surovegina[3], Vladimir Shashkin[3], Albert Davidov[4], Haiyan Tan[4], Louisa Meshi[4, 5], Alexander C. Pakpour-Tabrizi[6], Marie-Laure Hicks[6], and Richard B. Jackman[6]

Initial Hall Measurements

(vdp config.)

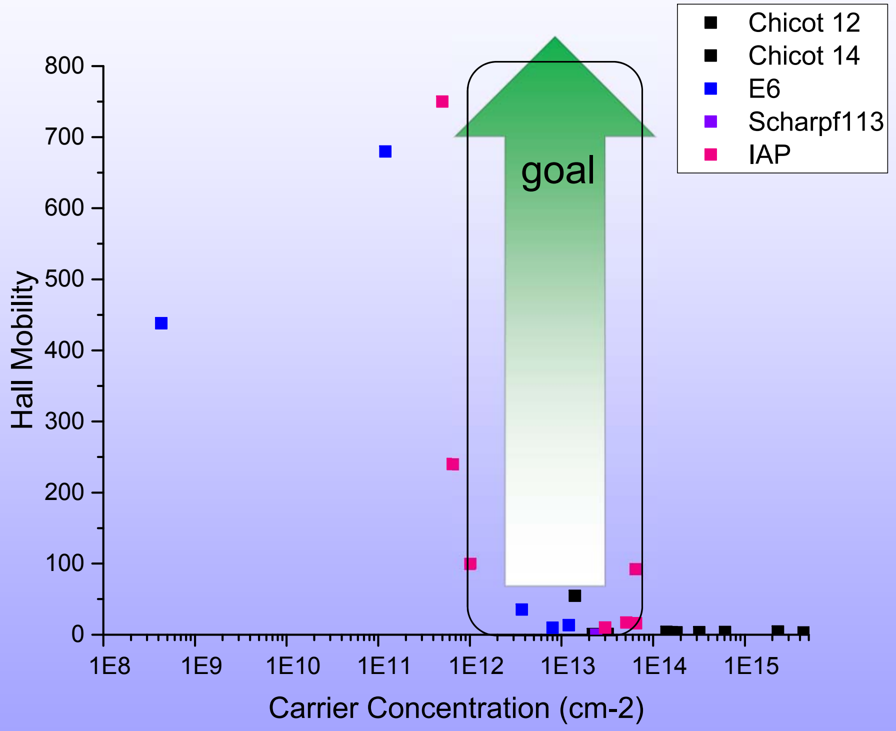

Summary

- Diamond Electronics is becoming a Reality!
- Why?
  - Available High Quality Substrates (HPHT)
  - High Purity Epitaxial Layer Growth (CVD)
  - Reliable Doping Methods
    - Traditional substitutional doping with B, P
    - H terminated surface conduction
    - Boron Delta Doping

- Thank You for Your Attention.

Acknowledgements

- Naval Research Laboratory – Office of Naval Research (1975-2010)
- Russian Science Foundation ‘Megagrant’ (2013-2017) Act 220 of Duma
- New Diamond Technology – St. Petersburg Russia